Observation of the associated production of a J/ψ meson with a W boson in pp collisions at $\sqrt{s} = 8$ TeV using the ATLAS detector

Rickard Lydahl

Thesis submitted for the degree of Bachelor of Science

Project duration: 2 months

Supervised by Else Lytken

Faculty of Science
Division of Particle Physics

January 20, 2016

LUND UNIVERSITY

Contents

Glossary ii

Abstract iii

Acknowledgements iv

Self-reflection v

Populärvetenskaplig sammanfattning vi

1 Introduction 1

2 Motivation and Theory 2
- 2.1 The Standard Model . . . 2
- 2.2 The J/ψ meson . . . 3
- 2.3 Associated production of a J/ψ with a vector boson . . . 3
- 2.4 Previous studies on J/ψ + W and J/ψ + Z production . . . 4

3 The Large Hadron Collider 5

4 A Toroidal LHC ApparatuS 6
- 4.1 Coordinate system and definitions . . . 7
- 4.2 The inner detectors . . . 8
- 4.3 Calorimeters . . . 8
- 4.4 Muon spectrometer . . . 9
- 4.5 Triggering . . . 9
- 4.6 Data set . . . 9

5 Method 10
- 5.1 Z boson candidate selection and reconstruction . . . 10
- 5.2 J/ψ + Z candidate strategy and selection . . . 11
- 5.3 J/ψ + W candidate strategy and selection . . . 12
- 5.4 Software tools and computing resources . . . 13

6 Results & Discussion 14
- 6.1 Z boson reconstruction and observation . . . 14
- 6.2 Observation of J/ψ + Z production . . . 15
- 6.3 Observation of J/ψ + W production . . . 17

7 Outlook 20

References 22

Glossary

ATLAS A Toroidal LHC ApparatuS. 6

DPS Double Parton Scattering. 4

ID Inner detector. 8

LHC Large Hadron Collider. 1

MC Monte Carlo. 14

QCD Quantum Chromodynamics. 2

SM Standard Model. 2

SPS Single Parton Scattering. 4

Abstract

Particle physics concerns the properties and interactions of the subatomic particles which make up our universe. Experiments typically consist of accelerating particles and colliding them together. Data of outgoing particles from the collision centre is acquired by detectors which translate particle properties into electronic signals. The experimental data is then analyzed and studied to probe theoretical predictions. The Large Hadron Collider was built outside Geneva and collides protons at the highest energy ever reached. Information about the collisions is then collected by several experiments such as the ATLAS experiment.

In this thesis the observation of the rare associated particle production of a J/ψ meson in association with a W boson is reported using 20.3 fb^{-1} of data from proton-proton collisions at $\sqrt{s} = 8$ TeV with the ATLAS detector. Currently, the way a J/ψ meson is produced at the Large Hadron Collider is not well understood and there are competing theories to describe this production. In combination with this analysis, the observation of a J/ψ meson in association with a Z boson, which is expected to have a lower production rate, is also done. A preliminary observation of the Z boson is done to familiarise with the analysis process. The Z boson reconstruction from the data is also compared with Monte Carlo simulation.

The observation of the particle productions are done using the dimuon decay channel for the Z boson and J/ψ meson. The W boson is reconstructed from a muon and a neutrino using the events missing energy. A total of 171 event candidates from $J/\psi + W$ production and 13 from $J/\psi + Z$ production are reported.

Acknowledgements

This work was made possible with the help and support of several people. First, I would like to thank my supervisor Else Lytken who was always active in helping me and giving me directions on how to continue my work. Next, I would like to thank Florido Paganelli who set up my workstation and gave me information and guidelines on how to handle the new work environment. To my office friends, Juno, Prim and Nicholai, I would like to thank you guys for being there and discussing physics problems and clearing up misunderstandings with me. Finally, I would like to thank my family who I love.

Self-reflection

The work performed in this thesis has improved my general physics knowledge in experimental particle physics data acquisition and particle production processes. In particular, my understanding of the methods and techniques used by researchers to search for experimental signatures with low production rate has improved from a very basic level. There were several times where my own searches for particle productions encountered problems that took long times to solve but which also helped me better understand the data analysis process and grow as a physicist.

This thesis introduced me to the many tools and programs which are commonly used in particle physics research. The work was performed via a Linux operating system on a cluster which you interact with through the terminal, all of which I had little to no experience with before. The experimental analysis was done using ROOT which interprets C++ code and can handle the large datasets which are used in particle physics. Getting familiar with both ROOT and C++ was a time-consuming process because they caused a majority of my struggles, but nevertheless a rewarding experience.

Working with a large dataset and submitting jobs on a cluster through bash scripts taught me the importance of how your code is created. Making your job task work in parallel instead of in series proved to be a very time saving process as the analysis time decreased from days to hours.

Populärvetenskaplig sammanfattning

Partikelfysik är läran om universums minsta beståndsdelar – elementarpartiklar. Teorin som sammanfattar alla kända elementarpartiklar kallas *Standardmodellen* och förklarar även hur dessa partiklar växelverkar med varandra. Växelverkan sker genom den elektromagnetiska, starka och svaga kraften samt Higgs mekanismen som ansvarar för partiklarnas massa. Standardmodellen är en mycket framgångsrik teori och har motstått flera experimentella studier och har även förutspått existensen av nya partiklar innan de upptäckts experimentellt. Standardmodellen ger dock inte svar på alla fenomen. I nuläget så har man bland annat inte kunnat inkorporera gravitationskraften i teorin. Det finns även andra fenomen som inte heller kan förklaras av teorin som oftast brukar klassificeras som *ny fysik*. I dessa fall letar man efter experimentella signaturer till nya teorier som, till exempel, supersymmetri, som då skulle breda vår kunskap om elementarpartiklarna.

Experiment i partikelfysik utgörs främst genom att accelerera partiklar till en hög energi och kollidera dem med varandra. I händelse av en partikelkollision så växelverkar partiklarna med varandra och nya, utgående, partiklar är bestämda med en viss sannolikhet. De två viktigaste parametrarna i ett kollisionsexperiment är energin av de inkommande partiklarna och *luminositeten*. Luminositet är definierat som det totala antalet kollisioner som äger rum under en viss tid. Att maximera luminositeten i ett kollisionsexperiment är oftast viktigt eftersom alla partikelproduktioner sker med en viss sannolikhet. En del partikel produktioner är väldigt sällsynta och för att kunna bekräfta dess händelse från en experimental signatur måste man se flera sådana händelser för att avvisa resultatet från statistiska fluktuationer.

Världens största partikelaccelerator, som både uppnår högst kollisionsenergi och luminositet, kallas för LHC (Large Hadron Collider). Den byggdes i CERN-laboratoriet utanför Genève där den accelererar två protonstrålar i motsatt riktning up till en designenergi av 7 TeV (teraelektronvolt) per proton. Protonstrålen är uppdelad i *bunches* av cirka en miljard protoner. En kollision sker när två bunches överlappar och protoner växelverkar med varandra. LHC har flera konstruerade kollisionspunkter där utgående partiklar detekteras och dess parametrar omvandlas till elektroniska signaler och samlas ihop i dataset. Den största partikeldetektorn vid LHC är ATLAS-experimentet som är cylindrisk och har en bredd på 44m och en diameter på 25m.

I den här avhandlingen så observeras två sällsynta dubbel partikel produktioner med ATLAS detektorn i en kollisionsenergi på 8 TeV. Den första observationen består av en J/ψ (J/psi) meson tillsammans med en Z boson från samma proton-proton kollision. En J/ψ meson kan växelverka med andra partiklar genom den starka och svaga kraften och är ett bundet tillstånd av två elementarpartiklar. En Z boson ansvarar för den svaga kraftens växelverkan och utgör en intressant partikelproduktion i association med en J/ψ meson. Den andra observationen som görs i denna avhandlingen är en J/ψ meson tillsammans med en W boson som också ansvarar för den svaga kraftens växelverkan. Dessa två observationer kan ge en starkare insikt in i produktionsmekanismen av en J/ψ meson vilket inte är fullt förstådd ännu.

I allmänhet så ser upptäckter av nya partiklar och dess växelverkan eller produktion inte någon direkt applikation till samhället utan framkommer mer genom spin-off teknologier. Detta är på grund av den experimentella partikelfysikens höga krav på teknologi som måste kunna tolka stora mängder data från partikelkollisioner. Den största spin-off tekniken som har sitt ursprung från partikelfysiksexperiment är den första webbläsaren och det så kallade *World Wide Web*.

1 Introduction

The scientific field of particle physics studies the properties and interactions of the most fundamental building blocks of our universe – elementary particles. The field has its roots in ancient Greece where the term 'atom' was coined by Democritus to describe the smallest, indivisible, unit of an element. Since then, theoretical and experimental advancement have shown that atoms are built up of electrons, protons and neutrons. Even further discoveries have been made showing that protons and neutrons are composites of three quarks, an elementary particle of which there are six flavours.

Most discoveries have occurred since the early 20th century. Initially, particle experiments were performed by studying cosmic rays, which are high-energy radiation from outer space. Cosmic rays entering Earth's atmosphere will interact with a particle and produce many secondary particles. Some of these particles will be able to reach Earth's surface before decaying and can therefore be studied. However, a more controlled experimental environment is usually needed to study more rare particle interactions. The first particle accelerators started appearing around the 1930's which could accelerate ions to a few hundred keV. The main concept is to use a high voltage electric field to accelerate a beam of charged particles in a high-vacuum beamline and either collide them into a fixed target or into another beam moving from the opposite direction. The latter is referred to as a collision experiment where one then surrounds the collision point with layers of detectors to study the outgoing particles.

The Large Hadron Collider (LHC) is a type of cyclic particle accelerator known as a synchrotron. It was built to expand current knowledge of particle physics and test new physics by achieving a collision energy never reached before. The process of creating outgoing particles from a collision is stochastic in nature and one therefore needs to collect data from a lot of collisions to be able to distinguish rare processes from statistical fluctuations. Such a rare process is the associated production of a J/ψ meson with a W boson which is the main focus of this thesis.

Elementary particles and their interactions with each other are described by the Standard Model of particle physics. Interactions are done through mediating particles called bosons and currently describe the electromagnetic, weak and strong forces. The W boson together with the Z boson mediate the weak force. The remaining particles of the Standard Model are fermions which are further divided into the sub-categories of leptons and quarks. The J/ψ particle is the bound state of a charm and anti-charm quark.

The J/ψ, together with the W and Z boson are short lived and can not be detected directly in a collision experiment. Therefore, one has to study the long-lived decay products of these particles which will interact with the detector. In this thesis, several particle observations are made with 20.3 fb^{-1} of data from $\sqrt{s} = 8$ TeV proton-proton collisions using the ATLAS detector at LHC. The first part of the work concerns the observation of the Z boson invariant mass in the decay channel $Z \to \mu^+\mu^-$.

Next, the rare process $J/\psi(\to \mu^+\mu^-) + Z(\to \mu^+\mu^-)$ is observed. This particle production has been observed before [1] at $\sqrt{s} = 8$ TeV proton-proton collisions with the ATLAS detector. Therefore, this work will be recreated here using a similar analysis method. Finally, the process $J/\psi(\to \mu^+\mu^-) + W(\to \mu\nu_\mu)$ will also be observed. It has previously been observed at a lower collision energy [2] with the ATLAS detector. This process contains a neutrino which will not directly be detected by ATLAS. Instead, the transverse components of the four-momentum vectors of all the particles in the event are summed up and flipped to point in the opposite direction. The final state consists of three muons

and missing transverse energy. The observed number of such processes is limited to the amount of data used from the proton-proton collisions.

2 Motivation and Theory

2.1 The Standard Model

The Standard Model (SM) of particle physics is a quantum field theory which classifies elementary particles and describes the electromagnetic, weak and strong interactions. Each elementary particle is described as an excitation to an underlying field. The theory has been developed since the 1960s when Sheldon Glashow discovered a way to combine the electromagnetic interactions and weak interactions into one unified theory [3]. Further developments were made in 1967 when the Higgs mechanism was incorporated into the theory by Steven Weinberg and Abdus Salam [4, 5]. Since then, the theory has withstood several stringent experimental tests and has predicted particles before their discovery.

The elementary particles are subatomic particles divided up into three groups: leptons, quarks and bosons. The leptons and quarks are fermions with spin 1/2 and obey the Pauli-exclusion principle. Fermions interact with other particles through bosons which themselves act as force mediators. A list of the known fermions and their basic properties is shown in Table 1. The bosons and the corresponding force carriers of the Standard Model are shown in Table 2. The listed particle masses are rounded values taken from the Particle Data Group [6]. Bosons with spin one are referred to as vector bosons which in the Standard Model are the four force carriers. Bosons with spin zero are called scalar bosons of which the Higgs boson is the only one in the Standard Model. The Higgs boson attributes mass to the other particles through their interactions with the Higgs field.

Table 1: The fermions of the Standard Model.

	Fermions	Short-hand	Charge	Mass
Quarks	up	u	+2/3	2.4 MeV
	down	d	-1/3	4.8 MeV
	charm	c	+2/3	1.27 GeV
	strange	s	-1/3	104 MeV
	top	t	+2/3	171.2 GeV
	bottom	b	-1/3	4.2 GeV
Leptons	electron	e	+1	0.511 MeV
	electron neutrino	ν_e	0	<2.2 eV
	muon	μ	+1	105.7 MeV
	muon neutrino	ν_μ	0	<0.17 MeV
	tau	τ	+1	1.77 GeV
	tau neutrino	ν_τ	0	<15.5 MeV

Quarks carry color charge which is a property of strong interactions and can therefore couple to gluons. The gluon itself also carries color charge and can interact with other gluons. The theory for strong interactions is called Quantum Chromodynamics (QCD) which aims to describe the complex nature between quarks and gluons. Together, three

Table 2: The Standard Model's five bosons.

Force	Boson	Charge	Mass	Spin
Electromagnetic	Photon	0	0	1
Weak	$W^{\pm}$, Z	± 1, 0	80.4 GeV, 91.2 GeV	1
Strong	Gluon	0	0	1
–	Higgs	0	125.09 GeV	0

quarks can create a bound state (qqq) known as a hadron and a quark and an anti-quark ($q\bar{q}$) can combine and produce a meson.

The weak force is mediated by the W and Z bosons and can change the flavour of quarks, *i.e.* change one type of quark into another. The weak force is also parity violating and can break CP-symmetry. The weak force carriers are heavy bosons that will decay in the order of $1 \cdot 10^{-24}$ seconds. This results in a projected range of $1 \cdot 10^{-18}$ metres for the weak force, a thousand times smaller than a nucleus.

2.2 The J/ψ meson

The J/ψ meson is the bound state of a charm quark with an anti-charm quark ($c\bar{c}$) and is a quarkonium particle which consists of a same-flavour quark and anti-quark pair combining into a flavourless meson. Other than J/ψ there are other bound states of a charm quark with an anti-charm quark making up the charmonium family. These particles can be represented as charmonium states in spectroscopic notation which can differ in total angular momentum, parity and charge parity. The first excited state of the J/ψ meson is the ψ' particle and it shares the same quantum numbers but differs in mass. This excitation is analogous to an orbital excitation of an electron in an atom. The J/ψ meson is a charge neutral particle with spin one and a has a world-average mass estimate of around 3.097 GeV/c^2. Similarly, the ψ' particle's mass is estimated to be 3.686 GeV/c^2. In this thesis, the observation of both a J/ψ and ψ' meson is reported.

2.3 Associated production of a J/ψ with a vector boson

Measurements of the production rate for the associated production of a J/ψ with a vector boson improves the calculation accuracy of quarkonium production models [7]. Currently, the two main competing theoretical models are the Color Singlet Model and Color Octet Model. In the Color Octet Model the production can only contribute at leading order and two possible Feynman diagrams of a W boson in association with a J/ψ are shown in Figure 1, where time flows from left to right. It is suggested that the color octet contributions dominate the total production rate [8].

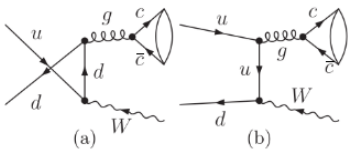

Figure 1: Color Octet Model leading-order J/ψ + W Feynman diagrams.

There have also been predictions that the associated production from next-to-leading-order Color Singlet Model contributions are also important [9]. A Feynman diagram of the first next-to-leading-order Color Singlet contribution to the $J/\psi + W$ production is shown in Figure 2. The process involves strange quark-gluon fusion which produces a W and charm quark. The charm quark then fragments into a J/ψ. Similar competing Feynman diagrams exists for J/ψ+Z production when comparing the Color Singlet Model and Color Octet Model.

The next-to-leading-order $J/\psi + W$ production at LHC (see Chapter 3) is calculated to be around 0.81 pb with a J/ψ transverse momentum larger than 10 GeV [8]. This low cross section is partly due to the large mass of the W boson, which requires a hard scattering process to occur to be created. The $J/\psi + Z$ production rate is also expected to be a factor lower due to the heavier mass of the Z boson.

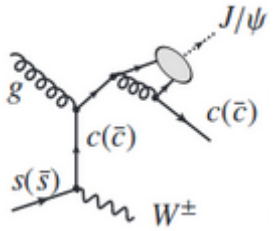

Figure 2: Color Singlet Model next-to-leading-order $J/\psi + W$ Feynman diagram.

2.4 Previous studies on $J/\psi + W$ and $J/\psi + Z$ production

Measurements on $J/\psi + W$ and $J/\psi + Z$ production are motivated by a few factors. The main goal is to better understand the production mechanism of quarkonia in hadron collisions, which is not fully understood. Other motivations include new physics searches where the associated production is the final decay state and a There have been several searches for associated particle production processes in proton-proton collisions with low production rate. A search for $W + \Upsilon(1S)$ and $Z + \Upsilon(1S)$ has previously been done with no evidence for its production, which set upper limits on the production rate [10]. The ATLAS searches for the associated particle production $J/\psi + W$ and $J/\psi + Z$, mentioned in Chapter 1 found signatures in excess of five standard deviations. These searches were conducted to probe the production mechanisms of quarkonium states in association with vector bosons. The $J/\psi + W$ measurement was done using the 2011 ATLAS dataset of 4.5 fb^{-1} from proton-proton collisions at a centre-of-mass energy of 7 TeV [2]. The J/ψ+Z search was done using 20.3 fb^{-1} of data from ATLAS proton-proton collisions at 8 TeV centre-of-mass energy [1].

A possible contribution to the production rate can come from non-prompt J/ψ, which originate from a b-hadron decay. Such events were taken into account in both analyses to produce a measurement of the cross-section for the production of a prompt J/ψ with a vector boson. Approximately 20–30% of the total production rate are expected to come from non-prompt J/ψ production. In addition to this contribution there is a possibility that the associated particle production can occur via a single parton (quark or gluon) scattering (SPS) or a double parton scattering (DPS). The angular distribution of the J/ψ and vector boson production in DPS is expected to differ from that of SPS. The extracted signal of the particle production did not distinguish between SPS and DPS in

both analyses. However, an estimate of the number of DPS events was made by taking into account the probability that a hard process (here a vector meson production) occurs together with another process (prompt J/ψ production) using a standard ansatz [11].

Possible background contribution for prompt J/ψ searches include multi-jet production and pileup which produces false signals. Pileup occurs when the desired signal is produced from two or more particle collisions in an event. The J/ψ + Z search observed $56 \pm 10 \pm 5$ events from prompt J/ψ production and $95 \pm 12 \pm 8$ events from non-prompt J/ψ production (the first error is statistical and the second systematic). The number of pileup events from prompt and non-prompt events were $5.2^{+1.8}_{-1.3}$ and $2.7^{+0.9}_{-0.6}$ respectively. The J/ψ + W search observed $29.2^{+7.5}_{-6.5}$ events from prompt J/ψ and $41.8^{+8.4}_{-7.3}$ events from non-prompt J/ψ production.

3 The Large Hadron Collider

The Large Hadron Collider (LHC) is a synchrotron used for proton-proton and heavy ion collisions [12] at CERN. A synchrotron is a cyclic particle accelerator which has a time-varying magnetic field used to guide the ions along the beamline. It was built outside Geneva, Switzerland and occupies the 26.7 km long tunnel which was previously used for the Large Electron-Positron collider. Figure 3 shows an aerial view of the border between Switzerland and France where the LHC is located. The main experiments are also shown, including ATLAS, CMS, ALICE and LHCb. The LHC proton-proton collision energy was

Figure 3: Aerial view of the LHC at CERN. The locations for the main experiments are shown.

designed to achieve collisions with a centre-of-mass energy of $\sqrt{s} = 14$ TeV and reach a luminosity of 10^{-34} cm^{2}s^{-1}. Previous runs on proton-proton collisions have been done at centre-of-mass energies of 7 TeV and 8 TeV. The current proton-proton centre-of-mass energy is at 13 TeV. The protons are produced by extracting hydrogen atoms from water molecules and stripping them of electrons. Before entering the LHC beamline the protons go through several acceleration stages at CERN's accelerator complex. Then, the protons are accelerated using an oscillating field known as a radio frequency electromagnetic field. Other than accelerating the protons it also splits the beam into bunches instead of maintaining a continuous beam.

The number of collision events N is related to the time integrated luminosity $\mathcal{L}$ and is given by:

$$N = \sigma\mathcal{L}, \tag{1}$$

where σ is the cross-section or probability for an interaction [13]. The luminosity is therefore defined as the number of particles that collide per unit area per unit time. The luminosity of a collider experiment is an important parameter and is optimized to its maximum value meaning there is more data to analyze. It is especially important when searching for processes with low production rates because larger luminosity increases the number of interesting events and the statistical significance. The luminosity is also proportional to the time two colliding particle bunches overlap. One defines an event in collider experiments as the outcome of a proton-proton collision being registered by the detector trigger system. It is possible that several bunches of protons collide in an event increasing the data acquisition. In the 8 TeV LHC run in 2012 the ATLAS detector (Chapter 4) collected 20.3 fb^{-1} of data from proton-proton collisions. This data is analyzed in this work which searches for the experimental signals mentioned in Chapter 1.

4 A Toroidal LHC ApparatuS

A Toroidal LHC ApparatuS (ATLAS) is a multi-purpose detector with cylindrical geometry located at one of the collision points of the LHC [14]. The detector consists of inner tracking detectors, calorimeters and a muon spectrometer, with the overall layout shown in Figure 4.

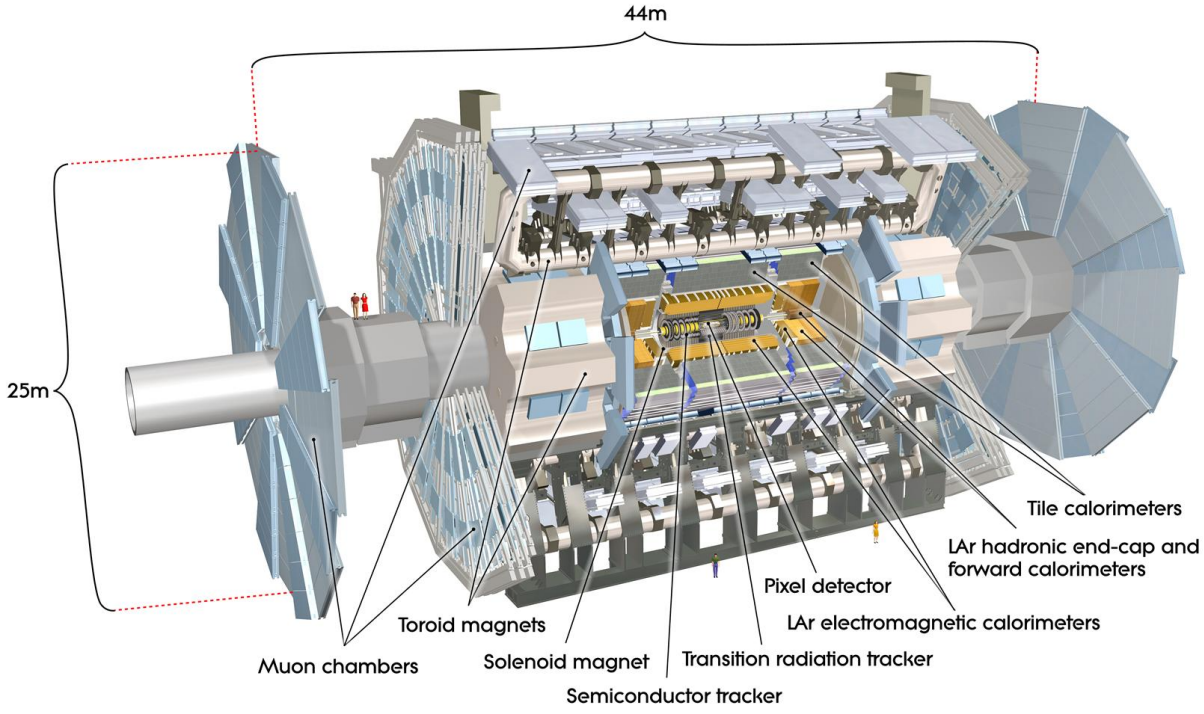

Figure 4: Schematic layout of the main ATLAS detector systems.

The inner detector is surrounded by a solenoid producing a 2 T magnetic field and performs particle tracking. A track is the reconstructed path a particle takes from the interaction point inferred through a series of detector position measurements. The electromagnetic and hadronic calorimeters give energy measurements of particles through absorption and is where most particles are stopped. Muons, however, mostly make it all the way through the detector and also interact with the muon detectors.

Neutrinos originating from the interaction point are not detected by any of the three detector layers. Collision events that contain neutrinos in the final state can be identified from the missing energy of that event. The missing energy is estimated by adding together the four-momentum vectors of all particles in the event and inverting its direction. This vector represents the neutrino present in the event and ensures momentum conservation.

4.1 Coordinate system and definitions

This section provides information and definitions necessary to study proton-proton collisions at the ATLAS detector. The ATLAS coordinate system has its origin in the nominal interaction point with the z-axis along the beam line. The x-y plane is therefore transverse to the beam direction. The positive x-axis points from the interaction point to the centre of the LHC ring and the positive y-axis points upward making it a right-handed coordinate system. Further, the azimuthal angle ϕ is the angle measured around the beam axis and the polar angle θ is the angle measured away from the beam axis, often called the emission angle. The transverse momentum is defined as the particle momentum in the x-y plane given by $p_T = p \sin\theta$.

To represent a particle's movement along the beam axis one defines the rapidity y and pseudo-rapidity η. Rapidity is measured along the beam axis and is defined as

$$y = \frac{1}{2} \ln \left[\frac{E + p_z c}{E - p_z c} \right], \tag{2}$$

where p_z is the momentum along the beam axis and E is the particle energy. Rapidity is an alternative to speed but differs in the fact that multiple velocities are additive in rapidity even at relativistic speeds. Pseudo-rapidity η is an approximation to rapidity that only has angular dependence and is defined as

$$\eta = -\ln \left[\tan \left(\frac{\theta}{2} \right) \right]. \tag{3}$$

If the particle velocity is close to c or if the emission angle θ is large then $y \approx \eta$. Calculating the pseudo-rapidity for a highly relativistic particle is often easier than rapidity because the total momentum vector is difficult to measure in this case.

One defines the distance between two particles ΔR in the pseudorapidity–azimuthal angle $(\eta - \phi)$ space as $\Delta R = \sqrt{(\Delta\eta)^2 + (\Delta\phi)^2}$. This definition will be used to check track isolation in the particle reconstruction.

In a collision experiment the primary vertex is chosen to be the vertex with the highest $\sum p_{\mathrm{T}}^2 / \mathrm{N}_{\mathrm{trk}}$, where $\mathrm{N}_{\mathrm{trk}}$ is the number of particle tracks. The impact parameter d_0 is defined in the transverse plane as the distance to the primary vertex. The expected resolution of the impact parameter is given by $\sigma(d_0)$ and the impact parameter significance is given by the ratio of the impact parameter with its resolution.

4.2 The inner detectors

The inner detectors (ID) are located closest to the collision point and consist of Pixel and silicon microstrip trackers surrounded by a Transition Radiation Tracker. These detectors allow measurements with high granularity which is necessary to be able to distinguish between particle tracks. It is estimated that in the region $|\eta| < 2.5$ around 1000 particles will emerge from the collision-point every 25 nanoseconds. This high track density is successfully resolved by the inner detector system. The dimensions of the inner detector system is around $2.1 \times 2.1 \times 6.2$ metres and it is surrounded by a solenoid producing a two Tesla magnetic field. The sensitive element in the Pixel detector is a "pixel" which has a resolution accuracy of around 0.05x0.03 millimetres. The particle path point-precision of the silicon microstrip detector is about 0.02 millimetres.

A particle that traverses through the pixel and silicon microstrip detectors will leave a series of hits that can be reconstructed into a particle track. The pixel and strip detector can achieve vertex and momentum measurements as well as pattern recognition and electron identification. Particles traversing the bulk of a silicon detector will ionise the silicon atoms producing free electrons. The bulk is a negatively doped region and the atoms that have an electron vacancy are referred to as "holes". The holes drift to a positively doped region in the detector and are collected and produce a measurable current on the strip. The electrons drift into a positively charged back plane. The detector consists of several strips and by determining which strip produced the electronic signal a high precision position measurement can be made.

The Transition Radiation Tracker consists of several tubes filled with gas mixtures and central straws. A potential is put across the tube and straw inducing an electric field. A charged particle that traverses the material between the tubes will emit photons. When the particle enters one of the tubes it will begin to ionize the gas, producing electron-ion pairs. The accompanying photons interact with molecules in the gas, producing more electrons. The electrons drift to the central straw while the ions drift towards the tube wall. The produced current from these charges gives information that a particle has passed through the tube. The amount of photons which are radiated, and therefore the number of electrons collected, differs between particles. It is therefore possible to distinguish between particles using the Transition Radiation Tracker.

4.3 Calorimeters

The ATLAS experiment has an electromagnetic calorimeter and hadronic calorimeter used to detect energy deposits of charged particles and hadronic particles, respectively, as they are absorbed by the calorimeter. The calorimeter system has a coverage in the pseudorapidity range $|\eta| < 4.9$ and is positioned outside the inner detectors. A charged particle that traverses the calorimeter system goes through electromagnetic or strong interactions in the active materials which are interlaced with an absorber. The active material in the ATLAS calorimeters is liquid argon, or plastic scintillators, which are interlaced with the absorbing materials.

A muon that traverses the calorimeter system will experience a small energy loss before entering the muon spectrometer. The energy lost by the muon is estimated by an algorithm that either uses a parametrised expected energy or the measured calorimeter energy. This effect is taken into account when muon tracks are reconstructed in the muon spectrometer and propagated back to the inner detector and interaction point.

4.4 Muon spectrometer

The Muon spectrometer is the outermost detector system of ATLAS and consists of Monitored drift tubes, Cathode strip chambers, Resistive plate chambers and Thin gap chambers. Muons are deflected by the large toroid magnet in the barrel region $|\eta| < 1.4$ and by two smaller magnets in the end-cap region $1.6 < |\eta| < 2.7$ and a combination of both in the transition region $1.4 < |\eta| < 1.6$. This magnetic field is mostly oriented at a right angle to the muon trajectories.

Precise position measurements are achieved using Monitored drift tubes over a pseudorapidity range $|\eta| < 2.7$. In the region $2.0 < |\eta| < 2.7$, Cathode strip chambers are also used to withstand the high particle rate and make high precision measurements. A muon is reconstructed by combining the track left in the inner detectors with the track in the muon system. The Resistive plate chambers and Thin gap chambers cover a region of $|\eta| < 1.05$ and $1.05 < |\eta| < 2.7$ respectively and are primarily used for triggering due to their fast decision time. The concept of triggering will be explained in Section 4.5.

A drift tube is based upon a wire chamber which is a type of proportional chamber that gives position measurements on incoming particles through electron-ion pair production in a gas. A drift tube differs in that one also measures the timing between pulses from different wires which consequently takes into account the drift time of ions moving to the closest wire in the chamber. This gives a more precise position measurement on the passing particle.

4.5 Triggering

In the $\sqrt{s} = 8$ TeV data taking period there were approximately 20.7 proton-proton interactions during every bunch crossing. Together with a bunch spacing of 25 nanoseconds there were around one billion collisions per second. Due to limitations in technology and resources, the data acquisition is limited to 200 events per second, a drastic decrease compared to the collision output.

Triggers are used to ensure that these 200 events per second contain interesting physics events. The trigger system contains three trigger levels (L1, L2 and event filter) which progressively refines the event selection by putting more stringent cuts. The L1 triggers work on hardware only and search for events with high transverse momentum leptons, photons, jets or large missing transverse energy. The L1 trigger level reduces the number of events to 75 kHz which are then transferred to the level two and event filter triggers. These are software triggers which further refine the level one cuts. Only a maximum of 200 events per second are passed through the level two and event filter triggers which will then be quality checked and reconstructed through data processing.

4.6 Data set

The data set used in this thesis work consists of muon events that have been identified using the `staco` algorithm [15] from the 8 TeV proton-proton collisions at ATLAS and was used for a previous lepton analysis [16]. The main property of the `staco` algorithm is that it reconstructs the muon track in the inner detector independently from the muon spectrometer and then combines them. The data was collected from a single-muon trigger which requires a muon with $p_{\mathrm{T}} > 18$ GeV. Further offline cuts have been made where at least one muon in the event must have $p_{\mathrm{T}} > 20$ GeV which ensures that we are looking at high transverse momentum events. The muon must also be in the pseudorapidity range

$|\eta| < 2.5$ which covers the inner detector and muon spectrometer. To avoid misidentification of muon tracks it is required that $Q_{\mathrm{ID}} = Q_{\mathrm{MS}}$, where Q_{ID} is the charge of the track left in the inner detector and Q_{MS} is the charge of the track left in the muon spectrometer.

On top of these basic selections there are a few more specific cuts. The muon track is required to be isolated in transverse momentum in a cone of size ΔR in the $\eta - \phi$ phase-space. Inside this cone the transverse momentum is set to be less than 7% of the total muon track p_{T} for the event to be accepted. Requirements on the impact parameter are also set to ensure that the muon originates close to the primary vertex. The transverse impact parameter significance is set to be $d_0/\sigma(d_0) < 3$, with $|d_0| < 0.2$ millimetres.

Muons that leave a track in both the ID and MS are referred to as "combined" muons and tracks that are identified in the inner detector and a segment of the muon spectrometer are called "segment-tagged" muons.

5 Method

The work performed in this thesis was done using 20.3 fb^{-1} of data collected with the ATLAS detector in proton-proton collisions at 8 TeV centre-of-mass energy. The tasks consists of performing the following observations:

1. Observation of Z boson invariant mass in the $\mathrm{Z} \to \mu^+\mu^-$ decay channel.
2. Observation of associated production $\mathrm{J}/\psi(\to \mu^+\mu^-) + \mathrm{Z}(\to \mu^+\mu^-)$.
3. Observation of associated production $\mathrm{J}/\psi(\to \mu^+\mu^-) + \mathrm{W}(\to \mu^\pm\nu)$.

The work is done using the muon data set described in Section 4.6 which already contains cuts on one muon. The selections done for the associated particle productions take into account the methods used in previous searches for $\mathrm{J}/\psi + \mathrm{Z}$ and $\mathrm{J}/\psi + \mathrm{W}$, which search for candidate events in the same decay channels [1, 2].

5.1 Z boson candidate selection and reconstruction

An initial four-momentum reconstruction of the Z boson from the decay channel $\mathrm{Z} \to \mu^+\mu^-$ is performed using the aforementioned data set using simple selection criteria. This is primarily done to get familiar with the selection and reconstruction processes before moving on to do more rigorous cuts necessary for the observation of the associated particle productions. The Z boson invariant mass spectrum is then observed from the data and compared with an ATLAS Monte Carlo simulation generated by ALPGEN-2.14 + HERWIG-6.520.

To observe $\mathrm{Z}(\to \mu^+\mu^-)$, events are required to have at least two identifiable muons. Muons from Z boson decays tend to have large transverse momentum and they are required to satisfy $p_{\mathrm{T}} > 25$ GeV. Further, muons are required to be in the range $|\eta| < 2.5$ to ensure good trigger efficiency and that they are identifiable in both the inner detector and muon spectrometer. Only muons which leave a track in both the ID and MS are considered (combined muons).

The four-momentum of the accepted muon candidates are reconstructed and two muon candidates four-momenta are added together. If the charges of the two muon candidates satisfy the decay $\mathrm{Z} \to \mu^+\mu^-$ then it is considered as a Z boson candidate. This selection only considers the two muon candidates with highest transverse momentum and does therefore not consider other possible muon combinations. Table 3 gives a summary of the selection criteria used in the reconstruction.

Table 3: Muon Requirements for $Z \to \mu^+\mu^-$ selection.

Z boson selection	
Transverse momentum	$p_T > 25$ GeV
Pseudorapidity	$\|\eta\| < 2.5$
Muon pair charge	0
Combined muon	TRUE

5.2 $J/\psi + Z$ candidate strategy and selection

The final state considered in this observation is $Z \to \mu^+\mu^-$ and $J/\psi \to \mu^+\mu^-$. Therefore, events with four or more muons are considered where two pairs of muons with opposite charge are combined. The invariant mass of the first selected muon pair is required to be close to the Z boson mass and, similarly, the invariant mass of the second pair needs to be close to the J/ψ mass. In both reconstructions the muon combination which is charge neutral and gives an invariant mass closest to the particle mass (J/ψ or Z) is considered. Muons that combine to a Z candidate are also not considered in the J/ψ selection and vice-versa. In cases where an event contains more than four muons all possible pairing combinations are considered up to six muons. This improves upon the selection process done in Section 5.1 and ensures that events with good candidates are not mistakenly rejected.

For muons to be considered candidates for Z boson reconstruction they are required to have $p_T > 15$ GeV and $|\eta| < 2.5$ and be combined muons. One of the muons must have $p_T > 25$ GeV to ensure high efficieny and is defined as the leading muon with the other accepted muon defined as the sub-leading particle. In addition, the muons are required to satisfy certain isolation criteria to distinguish against QCD jet background. The total sum of transverse momentum inside a cone of size $\Delta R = 0.2$ in the $\eta - \phi$ phase-space around the muon must be less than 15% of the muon transverse momentum. This calculation excludes the transverse momentum from the track associated with the muon. A reconstructed Z boson candidate must consist of an opposite-sign muon pair and have an invariant mass within 10 GeV of the world average Z boson mass: 91.1876 GeV/c^2. This mass window excludes many unwanted candidates while ensuring high acceptance for Z bosons. The width of the Z boson peak at half maximum is inversely proportional to its lifetime and is estimated to be 2.19 GeV.

Muons considered for J/ψ selection can either be segment-tagged or combined. At least one of the J/ψ muons must have $p_T > 4.0$ GeV and $|\eta| < 2.5$. Other muon candidates are required to have $p_T > 2.5$ with $1.3 < |\eta| < 2.5$ or $p_T > 3.5$ with $|\eta| < 1.3$. To be considered for a J/ψ + Z event the invariant mass of the J/ψ candidate must be within the mass range 2.6-3.6 GeV. This mass region ensures large J/ψ acceptance while being much smaller than the mass region given for Z boson acceptance. This is because the J/ψ meson has a characteristically long lifetime (short mass width) due to strongly suppressing hadronic decay modes because of the OZI rule.

Finally, the J/ψ candidate is also required to satisfy $8.5 < p_T^{J/\psi} < 100$ GeV and $|y^{J/\psi}| < 2.1$. The lower transverse mass limit and rapidity selection ensures J/ψ candidates with high acceptance and efficiency. The complete selection criteria for J/ψ + Z candidate selection are presented in Table 4.

Table 4: Requirements for $J/\psi(\rightarrow \mu^+\mu^-)$ + $Z(\rightarrow \mu^+\mu^-)$ selection.

Z boson selection	
Transverse momentum leading muon	$p_T > 25$ GeV
Transverse momentum sub-leading muon	$p_T > 15$ GeV
Pseudorapidity	$\lvert\eta\rvert < 2.5$
Candidate invariant mass	$\lvert m_{\mu^+\mu^-} - 91.1876\rvert < 10$ GeV
Track isolation momentum in cone $\Delta R < 0.2$	$< 0.15 p_{\mathrm{T}}$
Combined muon	TRUE
J/ψ meson selection	
$p_T(\text{leadingmuon}) > 4.0$ GeV	$\lvert\eta(\text{leading muon})\rvert < 2.5$ GeV
$p_T(\text{sub}-\text{leadingmuon}) > 2.5$ GeV	$1.3 <_{\lvert} \eta(\text{leading muon})\rvert < 2.5$ GeV
or $p_T(\text{sub}-\text{leadingmuon}) > 3.5$ GeV	$\lvert\eta\rvert < 1.3$
Combined or Segment-tagged muon	TRUE
Candidate invariant mass	$2.6 < m^{J/\psi} < 3.6$ GeV
Candidate transverse momentum	$8.5 < p_{\mathrm{T}}^{J/\psi} < 100$ GeV
Candidate rapidity	$\lvert y_{J/\psi}\rvert < 2.1$

5.3 $J/\psi + W$ candidate strategy and selection

The state considered in this selection is $J/\psi \rightarrow \mu^+\mu^- + W \rightarrow \mu^\pm\nu_\mu$ and therefore requires events to contain at least three identified muons. The muon pair that combines to a J/ψ candidate must be charge neutral, while the muon originating from a W decay is associated with the missing transverse energy $E_{\mathrm{T}}^{\mathrm{miss}}$ of the event. In events where several muon pairings are accepted as J/ψ candidates the same method stated in Section 5.2. is used, where the pair with invariant mass closest to the world average J/ψ mass is chosen. The muons that pass the W selection criteria are combined with the $E_{\mathrm{T}}^{\mathrm{miss}}$ and need to exceed a transverse mass threshold. If several muons satisfy this condition then the muon with highest transverse momentum is chosen to form the W candidate.

The W boson carries electric charge which prevents it from decaying into two charged leptons as was the case for the Z boson. Instead, the W boson can undergo a lepton decay satisfying charge conservation if the produced particles consists of a lepton and a neutrino. Since a neutrino is not expected to interact with the ATLAS detector, as mentioned in Chapter 4, one can not directly reconstruct the W boson invariant mass in this decay channel. Instead, one defines the transverse mass, m_{T}, which takes into account the missing transverse energy in the event. The $W(\rightarrow \mu\nu)$ transverse mass is defined as

$$m_{\mathrm{T}}(\mathrm{W}) = \sqrt{2p_{\mathrm{T}}(\mu)E_{\mathrm{T}}^{\mathrm{miss}}(1-\cos(\phi^{\mu}-\phi^{\nu_\mu}))} \tag{4}$$

where ϕ^{μ} and ϕ^{ν_μ} are the azimuthal angles of the muon and neutrino respectively as they emerge from the W boson decay. To accept a W boson candidate the event must fulfill $E_{\mathrm{T}}^{\mathrm{miss}} > 20$ GeV and $m_{\mathrm{T}}(\mathrm{W}) > 40$ GeV. The neutrino azimuthal angle is acquired from the direction of the missing energy vector which is reproduced by adding the vectors of all detected particles and inverting its direction.

Muons originating from a W boson are required to be combined muons and to have $p_{\mathrm{T}} > 25$ GeV and $\lvert\eta\rvert < 2.4$. The muon must be isolated in both E_{T} and p_{T} within a cone

of size $\Delta R = 0.3$ in $\eta - \phi$ phase-space around the muon. This isolation criteria is fulfilled if both parameters are less than 5% of the muon transverse momentum. Further, the W muon is required to satisfy $d_0/\sigma(d_0) < 3$ which, together with the isolation criteria, will reduce the acceptance of non-prompt muons originating from heavy flavour decays.

The J/ψ muon selection is done similarly to the selection set in Section 5.2. At least one J/ψ muon candidate is required to have $p_{\mathrm{T}} > 4.0$ GeV and $|\eta| < 2.5$ and otherwise muon candidates must have $p_{\mathrm{T}} > 3.5$ GeV with $|\eta| < 1.3$ or $p_{\mathrm{T}} > 2.5$ GeV with $1.3 < |\eta| < 2.5$ to be accepted. The muons can be either combined or segment-tagged. The J/ψ candidate is required to have $p_{\mathrm{T}}^{\mathrm{J}/\psi}$ in the region 8.5 to 30 GeV and $|y_{\mathrm{J}/\psi}| < 2.1$. The upper limit to the transverse mass improves the signal-to-background ratio as the signal is expected to decrease faster than background in terms of increasing transverse momentum. A complete listing of all J/ψ and W selections which are required to produce their associated particle production is shown in Table 5.

Table 5: Requirements for J/$\psi(\rightarrow \mu^+\mu^-)$ + W$(\rightarrow \mu^{\pm}\nu_{\mu})$ selection.

W boson selection	
Transverse momentum	$p_T > 25$ GeV
Pseudorapidity	$\|\eta\| < 2.4$
Transverse impact parameter significance	$d_0/\sigma(d_0) < 3$
Track isolation momentum in cone $\Delta R < 0.3$	$< 0.05 p_{\mathrm{T}}$
Combined muon	TRUE
Missing transverse energy	$E_{\mathrm{T}}^{\mathrm{miss}} > 20$ GeV
Transverse mass	$M_{\mathrm{T}}(\mathrm{W}) > 40$ GeV
J/ψ meson selection	
p_T(leadingmuon) > 4.0 GeV	$\|\eta$(leading muon)$\| < 2.5$ GeV
$p_T(\mathrm{sub-leadingmuon}) > 2.5$ GeV	$1.3 < \|\eta(\text{leading muon})\| < 2.5$ GeV
or $p_T(\mathrm{sub-leadingmuon}) > 3.5$ GeV	$\|\eta\| < 1.3$
Combined or Segment-tagged muon	TRUE
Candidate invariant mass	$2.5 < m^{\mathrm{J}/\psi} < 3.5$ GeV
Candidate transverse momentum	$8.5 < p_{\mathrm{T}}^{\mathrm{J}/\psi} < 30$ GeV
Candidate rapidity	$\|y_{\mathrm{J}/\psi}\| < 2.1$

5.4 Software tools and computing resources

The data analysis is created using ROOT, which is a framework that specialises in processing large amounts of data. ROOT has a built in C++ interpreter and introduces many useful classes and functions for statistical analysis, histograms and data storage. The data set consists of several ROOT files that are associated with different data taking periods of the ATLAS detector. Analysis of these data files are done by using the `TTree:MakeSelector` method which produces a code skeleton that is able to processes each event in the data. The selections given in Sections 5.1-5.3 were then written into separate code skeleton files using C++ language.

The analysis codes for the three different particle productions are located on a cluster environment. A Bash script was made that runs an analysis code and distributes the

workload on several nodes on the cluster. Each node will analyse a part of the data set and output a result, which can then be merged together with the other results. This method required the code to be able to run in parallel instead of in series to correctly allocate the workload on separate nodes. This effective use of computing resources resulted in an exponentially faster analysis time.

6 Results & Discussion

Here the observations of the Z boson and the associated production of a J/ψ meson with a weak vector boson are presented. The Z boson and J/ψ meson are reconstructed from the dimuon decay channel. To reconstruct the W boson, a muon is selected in association with the event's missing transverse energy, corresponding to the $W \to \mu\nu$ decay channel. The analysis is performed on the dataset discussed in Section 4.6, which contains high-p_{T} muons. The error bars on the data presented in this chapter represent statistical uncertainties only.

This chapter makes several references to the $J/\psi + W$ observation done with 4.5 fb^{-1} of data from ATLAS with 7 TeV centre-of-mass energy proton-proton collisions [2]. Similarly, many references are made to the $J/\psi + Z$ observation using proton-proton collisions at 8 TeV with 20.3 fb^{-1} of data from ATLAS [1].

6.1 Z boson reconstruction and observation

The Z boson invariant mass is reconstructed from the $Z \to \mu^+\mu^-$ decay channel following the muon selection given in Section 5.1. The Z boson candidates that passed all the selection criteria are shown in Figure 5. The plot shows the number of selected events per GeV/c^2 in the invariant mass region around the expected Z mass. A Monte Carlo simulation, which generates $Z \to \mu^+\mu^-$ events, is re-normalized to fit the data. The transverse momenta of the muons from the simulation have not undergone any smearing to fit the momentum resolution of the detector. This could be the cause of the small discrepancy between the data and Monte Carlo analysis seen in the figure.

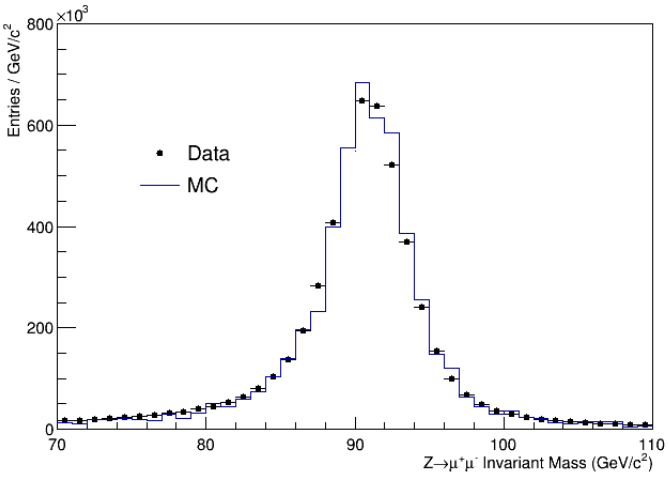

Figure 5: The Z invariant mass distribution from the decay channel $Z \to \mu^+\mu^-$. The data is shown in black dots and a Z boson Monte Carlo (MC) is normalized to the data in the region 70-110 GeV/c^2.

Due to there being no invariant mass restriction on the selected muon pairs, it was also possible to observe signatures of the J/ψ meson and excited ψ' state using the same decay channel. The invariant masses of the observed particle candidates are presented in Figure 6. Indications of the world-average mass estimates for the two mesons, previously stated in Section 2.2, are presented in the figure to show the good correspondence of the data with the expected signal.

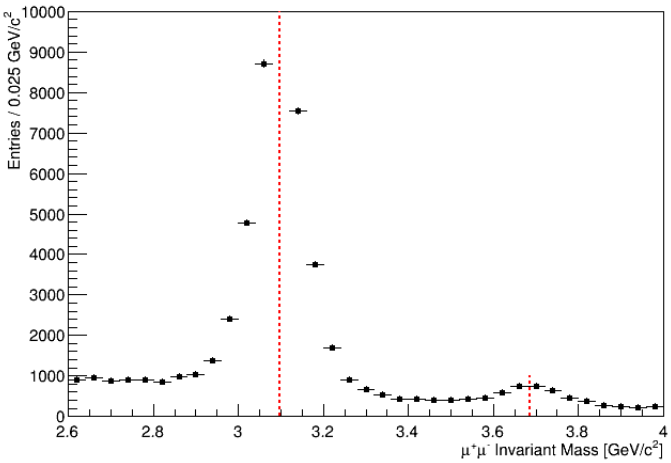

Figure 6: Invariant mass of $\mu^+\mu^-$ candidates indicating the presence of the J/ψ and ψ' particle. The red dotted lines indicate the world-average values for the J/ψ and ψ' particle.

Very little background is expected in the dimuon decay channel. Nevertheless, there is a possibility that other processes produce two muons with large transverse momenta. A significant part of the background is expected to be from a W decay into a muon and neutrino pair associated with a jet. A jet can either produce a fake muon signature or it contains real muons from decay processes. The possibility that a dijet event produces a fake signal is also present due to the large cross-section of QCD jets. The production of a top and anti-top quark pair that has two muons in its final decay state can also cause fake Z boson selections. Another possible background contribution is that the Z boson decays into a pair of tau leptons which subsequently decays into two muons to produce the signal. However, analysis of leptonic decay channels is the ideal choice for certain signals such as the Z boson.

To conclude this preliminary analysis, the results indicate that the standard cuts presented in Section 5.1 are sufficient to extract a signal for the Z boson and also the J/ψ and ψ' mesons. The dimuon invariant mass peaks show good agreement with the expected particle masses. The results also suggest that the acceptance for Z bosons is larger than for either J/ψ or ψ' with the chosen cuts. However, the cross section for J/ψ production is larger than Z boson production in proton-proton collisions at 8 TeV.

6.2 Observation of J/ψ + Z production

A scatter plot of the selected J/ψ+Z candidates is shown in Figure 7, where the invariant mass of the Z boson candidates is plotted against the invariant mass of the J/ψ candidates. A total of 13 candidate events were found which pass the selection criteria presented in

Section 5.2. Most of the candidates are concentrated around the expected J/ψ and Z masses indicated by the red dotted lines.

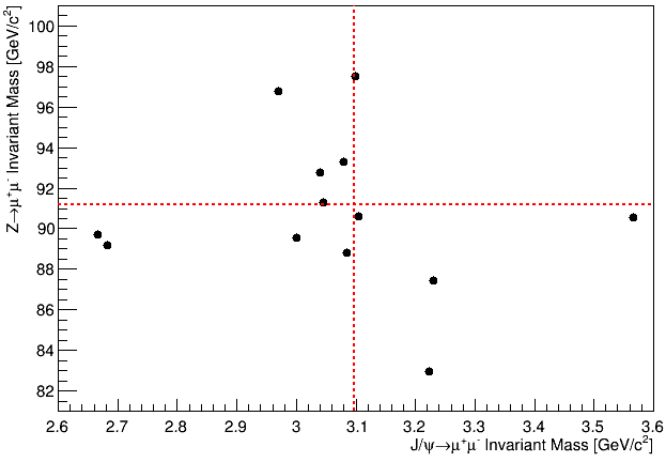

Figure 7: The selected J/ψ + Z candidates in the Z invariant mass versus J/ψ invariant mass plot. The red dotted lines indicate the world-average masses of the particles.

The selection does not distinguish between prompt and non-prompt J/ψ production, which therefore includes background from the production of a Z boson with a b-hadron in the signal. This could suggest that the analysis does not show a statistically significant yield of Z + prompt J/ψ candidates since the expected production rate for non-prompt J/ψ is expected to be 20-30%. Other background contributions can originate from pileup and double parton scattering (DPS) which are not distinguished against in the selection. The possibility for DPS contribution is present for events with both prompt and non-prompt J/ψ production. The number of DPS events can be estimated from the effective cross-section for double parton interaction which has previously been measured in W + 2-jet events by ATLAS [17], and the cross sections from prompt and non-prompt J/ψ production.

The J/ψ and Z invariant mass distributions are shown in Figure 8, and Figure 9, respectively. The small number of candidates indicate peaks around the expected masses with large statistical errors. Extracting a signal from this limited amount of candidates could not show significant excess in events that correspond to a J/ψ + Z signature. The previous observation of this associated particle production acquired a yield of $56 \pm 10 \pm 5$ events from prompt J/ψ production and $95 \pm 12 \pm 8$ events from non-prompt J/ψ production and used the same proton-proton collision energy and luminosity from the ATLAS experiment [1]. This discrepancy in candidate yield presented here could be due to the extra tight cuts imposed on the muons from the data set which could exclude J/ψ + Z candidates.

The Z boson selection sets a lower transverse momentum limit on one of the muon candidates, assuring a higher Z boson acceptance compared to the selections made in Section 5.1. Further, an isolation criterion was set on the muon candidates to eliminate background from multi-jet production which can reproduce several high-p_{T} muons. The selected Z boson was reconstructed from the muon combination that had an invariant mass closest to the world-average Z mass and had neutral charge. The same pair formation technique was imposed on the muons making up the J/ψ candidate. Here, tighter cuts were made on the muon pair in $p_{\mathrm{T}}^{\mathrm{J}/\psi}$ and $y_{\mathrm{J}/\psi}$. With no isolation criteria, multi-jet

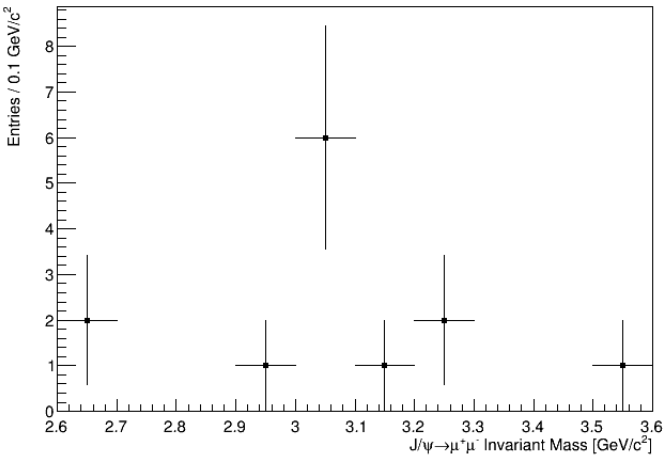

Figure 8: J/ψ invariant mass distribution in the selected mass region 2.6-3.6 GeV from the associated production of a J/ψ meson with a Z boson.

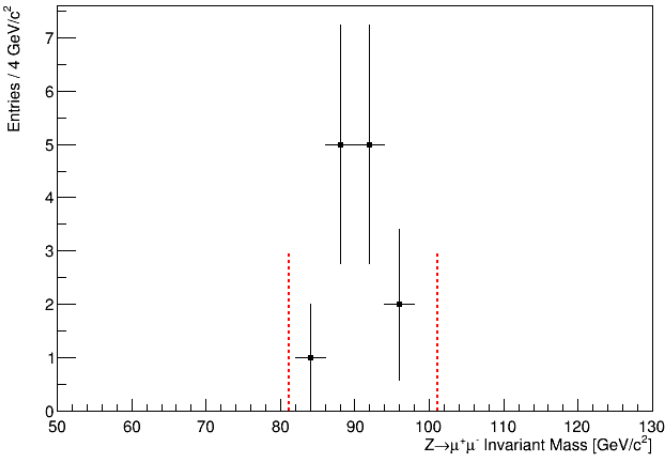

Figure 9: Invariant mass distribution of Z candidates from the associated production of a J/ψ meson with a Z boson. The red dotted lines indicates the accepted mass region: $|m_{\mu^+\mu^-} - 91.1876| < 10$ GeV.

background is, however, expected to contribute to the signal. The J/ψ candidate's large range in transverse momentum from 8.5-100 GeV ensures high acceptance of candidates, including fakes. Due to the presence of background in both particle reconstructions it is possible that the J/ψ is paired with a fake Z candidate and vice-versa.

6.3 Observation of J/ψ + W production

The transverse mass distribution of the W boson in the W $\rightarrow \mu\nu$ decay channel is shown in Figure 10. Events were required to have at least three muons. This reconstruction has passed all the W boson requirements given in Section 5.3, but omits the requirements for the associated J/ψ + W production, consequently excluding the J/ψ reconstruction. The transverse mass was calculated according to Equation 4, which gives a wide distribution with a feature often called the Jacobian peak at the W boson mass.

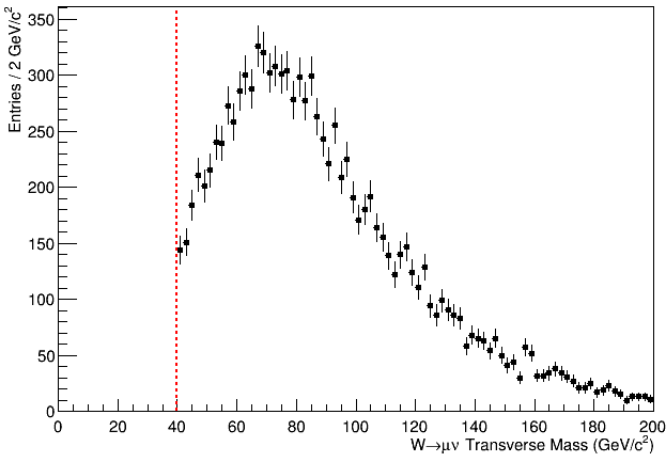

Figure 10: Transverse mass distribution of all selected W($\rightarrow \mu\nu$) boson candidates (black dots) in events containing three or more muons. The red dotted line indicates the cut at $m_{\mathrm{T}}(\mathrm{W}) = 40$ GeV.

A scatter plot of the selected J/ψ+W candidates is shown in Figure 11. In total, there were 171 candidate events observed in the selected mass region with a large concentration of candidates around the J/ψ mass. This high concentration indicates that a tighter cut on the mass of the J/ψ candidates is possible in future studies. The wide distribution in transverse momentum is in agreement with Figure 10. The 7 TeV ATLAS analysis was left with 149 events after the selection and uses some tighter cuts. Like stated in the previous section, this discrepancy could be due to the tight cuts imposed on the muons from the data set.

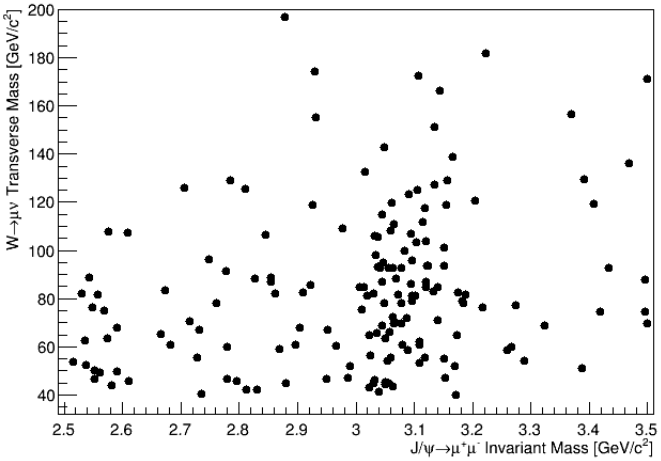

Figure 11: The selected J/ψ+W candidates in the W transverse mass versus J/ψ invariant mass plot.

Figure 12, shows the invariant mass distribution of J/ψ candidates from the dimuon decay channel. The cuts are consistent with the J/ψ selection made in the J/ψ+Z search, except for a tighter suppression on $p_{\mathrm{T}}^{\mathrm{J}/\psi}$. A peak can clearly be identified around the expected mass, suggesting that the selection is consistent. From the J/ψ reconstruction

there were 49 cases where more than one muon-pair combination gave an invariant mass within the region 2.5-3.65 GeV.

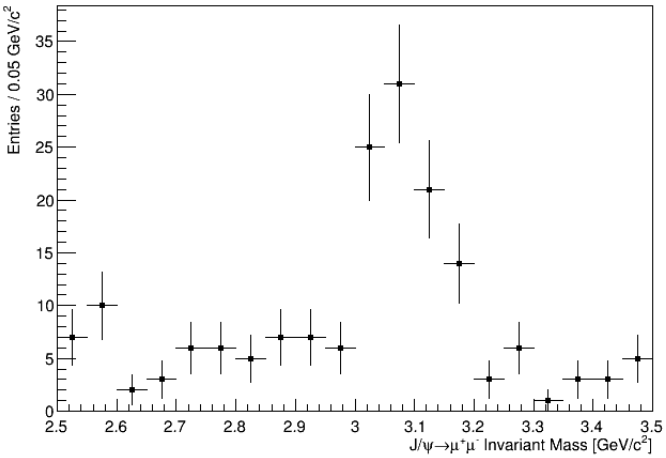

Figure 12: Invariant mass distribution of selected J/$\psi(\rightarrow \mu^+\mu^-)$ candidates from the associated J/ψ + W particle production.

Figure 13 shows the transverse mass distribution of a W boson produced from a muon and a neutrino. The distribution is consistent with Figure 10 and shows the characteristic wide peak associated with a W boson.

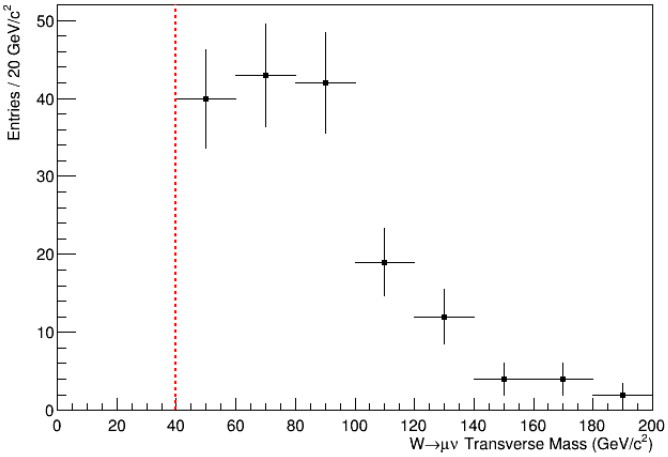

Figure 13: Transverse mass distribution of selected W$(\rightarrow \mu\nu)$ boson candidates from the associated J/ψ + W particle production.

There are several possible background events that can contribute to the signal. First, there is a possibility for W + non-prompt J/ψ production from the associated production of a W boson with a b quark. This process has been discussed in previous sections and is not distinguished against in the candidate selection. There is also a possibility that the signal is produced from double parton scattering in the proton-proton collision. Another background contribution is expected from multi-jet events which can result in fake signals.

A possible decay of $B_c \rightarrow$ J/$\psi\mu^{\pm}\nu_{\mu}X$ produces a J/ψ with a muon and a neutrino that mimics the signal. This effect is taken to be very small as no such possible candidates were found in the 7 TeV ATLAS search.

There is a possibility that the signal can originate from a Z boson. This can be checked for by combining the muon originating from the W with the two J/ψ muons. If a neutral pair is formed with an invariant mass in the region $|m_{\mu^+\mu^-} - 91.1876| < 10$ GeV it could suggest that a fake signal is produced. These events can be omitted but the effect was not taken into account for in this analysis.

7 Outlook

The work done in this thesis presents the observation of the associated production of a J/ψ meson with a W or Z boson. Here, observation is defined simply as a visible peak and does not take into account the statistical significance of the signal. A preliminary observation was also done on the Z boson to become familiarized with the event reconstruction process. The analysis was done on proton-proton collisions at 8 TeV centre of mass energy using 20.3 fb^{-1} of data from the ATLAS detector. The J/ψ meson and Z boson were searched for in the dimuon decay channel and the W boson was searched for in the W $\rightarrow \mu\nu$ decay channel. A total of 13 candidates were observed of the production of a J/ψ meson in association with a Z boson. For the associated production of a J/ψ meson with a W boson, a total of 171 candidates were observed.

After the observation of the two associated particle production, the next step would be to extract a signal from the candidate events using a fit model and calculate the statistical significance of the signal. The observed candidate events of the associated particle productions arise from a number of signal and background sources already discussed. One would therefore like to evaluate the contributions from these sources to the total number of candidate events observed.

It is possible to separate the prompt and non-prompt J/$\psi(\rightarrow \mu^+\mu^-)$ candidates into two categories by looking at the pseudo-proper time distribution together with the invariant mass distribution of the J/ψ candidates. The pseudo-proper time τ is defined as

$$\tau = \frac{\mathbf{L} \cdot \mathbf{p}_{\mathrm{T}}^{\mathrm{J}/\psi}}{p_{\mathrm{T}}^{\mathrm{J}/\psi}} \cdot \frac{m^{\mathrm{J}/\psi}}{p_{\mathrm{T}}^{\mathrm{J}/\psi}} \tag{5}$$

where $\mathbf{L}$ is the separation vector between the primary vertex and the J/ψ decay vertex. The prompt J/ψ candidates would have a pseudo-proper time of zero, distributed around this value due to finite detector resolution. Non-prompt J/ψ candidates have decay vertices that are displaced from the primary vertex and will therefore have positively distributed pseudo-rapidity values. By applying a fit model to the associated particle production one can estimate the number of candidates that result from prompt and non-prompt J/ψ mesons. This check would distinguish against the associated productions of a weak vector boson and a bottom quark, where the bottom quark handronises and subsequently decays into a J/ψ. The prompt and non-prompt signals still contain background contributions which can be included in the fit model, which is not trivial.

To perform a calculation of the pseudo-proper time it is necessary to reconstruct the vertex of the J/ψ candidate, which was not done. If the work was done again, then extra care needs to be taken to reconstruct the decay vertices, so that future signal extraction can be done and prompt and non-prompt J/ψ candidates can be distinguished. It is also possible to exclude a large portion of background events from pileup by restricting the separation of the J/ψ vertex and Z vertex (in the J/ψ + Z search) along the beam axis.

In the ATLAS data taking period for proton-proton collisions used in this analysis, an estimate of 20.7 proton-proton interactions occur at every bunch crossing. From these interactions there is a possibility that more than one proton-proton hard scattering occurs, which can produce the desired signal.

To perform a more thorough analysis, if re-doing the work, the search for $J/\psi + Z$ would be omitted to dedicate more time to the $J/\psi + W$ analysis. The proton-proton cross section for the associated production of an J/ψ meson with a Z boson is measured to be lower than $J/\psi + W$ production [1, 2], setting stringent cuts on the event selection, making it a more difficult task. The $J/\psi + W$ analysis also shows more variety in physics and signal extraction, namely, the concept of associating a neutrino with the missing energy of an event. Nevertheless, the observations done in this thesis work show the strength of the LHC and ATLAS detector in producing large amounts of data to study rare particle productions.

References

[1] ATLAS Collaboration. Observation and measurements of the production of prompt and non-prompt J/ψ mesons in association with a Z boson in pp collisions at $\sqrt{s} =$ 8 TeV with the ATLAS detector. *Eur. Phys. J.*, C75(5):229, 2015.

[2] ATLAS Collaboration. Measurement of the production cross section of prompt J/ψ mesons in association with a $W^{\pm}$ boson in pp collisions at $\sqrt{s} = 7$ TeV with the ATLAS detector. *JHEP*, 04:172, 2014.

[3] Sheldon L. Glashow. Partial-symmetries of weak interactions. *Nuclear Physics*, 22(4):579 – 588, 1961.

[4] Steven Weinberg. A model of leptons. *Phys. Rev. Lett.*, 19:1264–1266, Nov 1967.

[5] A. Salam. Weak and electromagnetic interactions. 1969. Proc. of the 8th Nobel Symposium on 'Elementary particle theory, relativistic groups and analyticity', Stockholm, Sweden, 1968, edited by N. Svartholm, p.367-377.

[6] K. A. Olive et al. Review of Particle Physics. *Chin. Phys.*, C38:090001, 2014.

[7] Song Mao, Ma Wen-Gan, Li Gang, Zhang Ren-You, and Guo Lei. QCD corrections to J/ψ plus Z^0-boson production at the LHC. *JHEP*, 02:071, 2011. [Erratum: JHEP12,010(2012)].

[8] Gang Li, Mao Song, Ren-You Zhang, and Wen-Gan Ma. QCD corrections to J/ψ production in association with a W-boson at the LHC. *Phys. Rev.*, D83:014001, 2011.

[9] J. P. Lansberg and C. Lorce. Reassessing the importance of the colour-singlet contributions to direct $J/\psi + W$ production at the LHC and the Tevatron. *Phys. Lett.*, B726:218–222, 2013. [Erratum: Phys. Lett.B738,529(2014)].

[10] CDF Collaboration. Search for associated production of υ and vector boson in $p\overline{p}$ collisions at $\sqrt{s} = 1.8$ TeV. *Phys. Rev. Lett.*, 90:221803, Jun 2003.

[11] N. Paver and D. Treleani. Multi - Quark Scattering and Large p_T Jet Production in Hadronic Collisions. *Nuovo Cim.*, A70:215, 1982.

[12] Lyndon Evans and Philip Bryant. Lhc machine. *Journal of Instrumentation*, 3(08):S08001, 2008.

[13] Werner Herr and Bruno Muratori. Concept of luminosity. 2006.

[14] The ATLAS Collaboration. The atlas experiment at the cern large hadron collider. *Journal of Instrumentation*, 3(08):S08003, 2008.

[15] R. Nicolaidou, L. Chevalier, S. Hassani, J. F. Laporte, E. Le Menedeu, and A. Ouraou. Muon identification procedure for the ATLAS detector at the LHC using Muonboy reconstruction package and tests of its performance using cosmic rays and single beam data. *J. Phys. Conf. Ser.*, 219:032052, 2010.

[16] A. Hawkins. *Search for beyond Standard Model physics with same-sign dileptons*. PhD thesis, Lund University, Lund, 2014.

[17] Georges Aad et al. Measurement of hard double-parton interactions in $W(\rightarrow l\nu)+2$ jet events at $\sqrt{s}$=7 TeV with the ATLAS detector. *New J. Phys.*, 15:033038, 2013.